Climate Response to External Sources of Freshwater: North Atlantic versus the Southern Ocean

RONALD J. STOUFFER

Geophysical Fluid Dynamics Laboratory, Princeton, New Jersey

DAN SEIDOV AND BERND J. HAUPT

The Pennsylvania State University, University Park, Pennsylvania

(Manuscript received 26 January 2006, in final form 21 June 2006)

ABSTRACT

The response of an atmosphere–ocean general circulation model (AOGCM) to perturbations of freshwater fluxes across the sea surface in the North Atlantic and Southern Ocean is investigated. The purpose of this study is to investigate aspects of the so-called bipolar seesaw where one hemisphere warms and the other cools and vice versa due to changes in the ocean meridional overturning. The experimental design is idealized where 1 Sv (1 Sv $\equiv 10^6$ m^3 s^{-1}) of freshwater is added to the ocean surface for 100 model years and then removed. In one case, the freshwater perturbation is located in the Atlantic Ocean from 50° to 70°N. In the second case, it is located south of 60°S in the Southern Ocean.

In the case where the North Atlantic surface waters are freshened, the Atlantic thermohaline circulation (THC) and associated northward oceanic heat transport weaken. In the Antarctic surface freshening case, the Atlantic THC is mainly unchanged with a slight weakening toward the end of the integration. This weakening is associated with the spreading of the fresh sea surface anomaly from the Southern Ocean into the rest of the World Ocean. There are two mechanisms that may be responsible for such weakening of the Atlantic THC. First is that the sea surface salinity (SSS) contrast between the North Atlantic and North Pacific is reduced. And, second, when freshwater from the Southern Ocean reaches the high latitudes of the North Atlantic Ocean, it hinders the sinking of the surface waters, leading to the weakening of the THC.

The spreading of the fresh SSS anomaly from the Southern Ocean into the surface waters worldwide was not seen in earlier experiments. Given the geography and climatology of the Southern Hemisphere where the climatological surface winds push the surface waters northward away from the Antarctic continent, it seems likely that the spreading of the fresh surface water anomaly could occur in the real world.

A remarkable symmetry between the two freshwater perturbation experiments in the surface air temperature (SAT) response can be seen. In both cases, the hemisphere with the freshwater perturbation cools, while the opposite hemisphere warms slightly. In the zonally averaged SAT figures, both the magnitude and the pattern of the anomalies look similar between the two cases. The oceanic response, on the other hand, is very different for the two freshwater cases, as noted above for the spreading of the SSS anomaly and the associated THC response.

If the differences between the atmospheric and oceanic responses apply to the real world, then the interpretation of paleodata may need to be revisited. To arrive at a correct interpretation, it matters whether or not the evidence is mainly of atmospheric or oceanic origin. Also, given the sensitivity of the results to the exact details of the freshwater perturbation locations, especially in the Southern Hemisphere, a more realistic scenario must be constructed to explore these questions.

1. Introduction

The ocean thermohaline circulation (THC) is conventionally defined as the part of the ocean's circulation that consists of relatively warm, saline surface waters flowing northward in the Atlantic basin to high northern latitudes. In the high latitudes of the North Atlantic, the surface waters are strongly cooled by the atmosphere, causing them to become dense enough to sink to great depths. The dense, deep waters flow southward out of the Atlantic basin and into the Southern Ocean, where they mix with the rest of the World

Corresponding author address: Ronald J. Stouffer, Geophysical Fluid Dynamics Laboratory, Princeton, NJ 08542.
E-mail: ronald.stouffer@noaa.gov

Ocean water masses. The present-day state of THC is that it is a global water circulation system connecting very distant regions of the World Ocean.

Since the THC circulation involves relatively warm surface water flowing northward and relatively cold deep water flowing southward in the Atlantic Ocean, a large amount of heat is transported toward the high northward latitudes. This heat flux warms the Northern Hemisphere (NH), by "stealing" or "pirating" heat from the Southern Hemisphere (SH; e.g., Crowley 1992; Stocker 1998; Seidov and Maslin 2001). A strengthening of the flow would tend to warm the NH and cool the SH. A weakening of the flow would have the opposite effect. Changes in the THC strength thus have the potential to produce a bipolar seesaw in the temperature anomalies (Broecker 1998).

Using proxy temperature estimates derived from ice cores, a number of authors have found such a bipolar seesaw and have noted an out-of-phase temperature anomaly relationship between Greenland and the Antarctic (e.g., Blunier and Brook 2001). The out-of-phase relationship between the temperature anomalies of the two hemispheres is not simple, in the sense that there seem to be time lags in the relationship (Steig and Alley 2002; Schmittner et al. 2003). Recently Stocker and Johnsen (2003) proposed a simple thermodynamic model that introduces a heat reservoir in the Southern Ocean, which seems to be able to explain many of the time lags and phasing of the temperature anomalies inferred from the ice record.

Crowley (1992) and Stocker et al. (1992) noted that changes in the strength of the THC would lead to warming of one hemisphere while the other cools—a bipolar seesaw in temperature anomalies. On the other hand, Broecker (1998, 2000) relates changes in the Atlantic THC to deep ocean ventilation in the two hemispheres, where a weakening of the Atlantic THC would lead to a strengthening of Antarctic Bottom Water (AABW) formation and vice versa. The changes in deep ocean ventilation would lead to changes in the amount of heat being released to the overlying atmosphere. A weakening of the North Atlantic Deep Water (NADW; and associated Atlantic THC) would reduce the warming of the atmosphere in the NH, while the increase of the AABW would warm the SH.

As noted by Rahmstorf (2002), both these two hypotheses can lead to bipolar seesaws in the temperature anomalies. The modeling studies of Manabe and Stouffer (1988, 1999), Vellinga and Wood (2002), and Rind et al. (2001) demonstrate that the two hypotheses are closely related. The heat transported northward by the Atlantic THC is mainly ventilated to the atmosphere via deep-water formation events.

Other authors have postulated much more complex oscillation regimes to explain the bipolar relationship in temperature anomalies between the two hemispheres, including potential lead–lag relationships with the land ice masses (e.g., Steig and Alley 2002; Clark et al. 2002). The timing of the feedbacks of the oscillation is not the subject of this study because of its idealized design and relatively short integration time scales (200 model years). Here we investigate the impact of an idealized source of meltwater from the land ice mass in either hemisphere on the oceanic circulation and climate on a century time scale.

A number of models, atmosphere–ocean general circulation models (AOGCMs) and simpler models, have been used to explore the climate response to large freshwater inputs in high latitudes of the North Atlantic Ocean (e.g., Manabe and Stouffer 1995; Ganopolski and Rahmstorf 2001; Rind et al. 2001; Vellinga and Wood 2002; Weaver et al. 2003; Knutti et al. 2004; Stouffer et al. 2006). These results show that the North Atlantic THC weakens in response to the additional freshwater applied at the ocean surface in high latitudes of the North Atlantic. If the freshwater perturbation rate is large enough, some model results indicate that it is possible for the THC to change stable states—from the current "on" mode to an "off" mode (e.g., Manabe and Stouffer 1999; Stouffer et al. 2006). The on mode is characterized by an overturning circulation similar to that found in present-day observations of the Atlantic Ocean. In the off mode, this circulation is absent.

In these model experiments, the reduction of northward heat transport and associated oceanic deep convection leads to a decrease of the North Atlantic sea surface temperatures (SSTs) and surface air temperatures (SATs). The weakening of the THC is a result of the freshwater reducing the density of the surface waters inhibiting the vertical circulations (convection and advection). The reduction of oceanic convection, which brings warmer subsurface waters to the ocean surface, also leads to a cooling of the surface waters. The decrease of the horizontal and vertical heat transports results in a strong surface cooling locally and can result in a hemispheric cooling if the rate of this decrease is large enough (Manabe and Stouffer 1997; Vellinga and Wood 2002).

The longer residence times of the surface waters in the high latitudes of the North Atlantic are an additional positive feedback to the weakening of the THC caused by freshwater capping (Manabe and Stouffer 1995). High latitudes are regions where the surface fluxes normally cool and freshen the ocean surface. The longer residence times of the North Atlantic surface waters means they experience the atmospheric cooling

and freshening longer than in the case of faster or stronger THC—the surface freshening is a positive feedback on the THC weakening.

Can freshwater inputs in the Southern Ocean lead to a strengthening of the Atlantic THC when the THC is in its on mode? A few modeling studies have been conducted to investigate this hypothesis. Using an ocean-only model, Seidov et al. (2001) imposed a freshwater anomaly [through changes in the restored sea surface salinity (SSS)] in both hemispheres. They found that the THC (and associated northward heat transport) in the Atlantic decreased when the North Atlantic SSS was reduced. They also found that the Atlantic THC increased when the Southern Ocean SSS was decreased. However, these results were questioned in recent work by Seidov et al. (2005), who found that because of specific geometry of the Southern Ocean, freshening, or more generally "de-densification" of the Southern Ocean surface water does not result in a densification in the northern North Atlantic surface waters. They found that lighter water tends to escape the Southern Ocean and spread over the entire World Ocean. This spreading is further investigated in this paper.

In addition, a series of new experiments (Seidov and Haupt 2003, 2005; Saenko et al. 2004) show that the density contrast between the Atlantic and Pacific Oceans imposes perhaps a stronger control over THC than northern–southern de-densifications, at least on longer time scales. In view of all these results, it is possible that the mechanisms involved in producing the bipolar surface temperature seesaw may be more complex than previously thought.

Weaver et al. (2003), using a simple coupled model where the ocean component is an ocean general circulation model (OCGM) and the atmosphere component is an energy balance model, investigated the climatic response to freshwater inputs in both hemispheres. In integrations where the Atlantic THC is absent (or off), they add freshwater just north of the Antarctic Circumpolar Current (ACC) and in a second experiment they add freshwater near Antarctica. In both cases, they found that the Atlantic THC strengthened, switching from an off to an on state. The THC changes lead to warming in the Northern Hemisphere in response to the freshening of the Southern Ocean. These results will be discussed further in section 4 of this paper.

Here we use an AOGCM (Delworth et al. 2002) to study the climate's response to freshwater in the North Atlantic and Southern Ocean. This model has been designed for climate change studies and was state-of-the-art in the mid-1990s (Cubasch et al. 2001). Because of the cost of conducting the integrations presented here, we perform only two idealized perturbation experiments. In one, the North Atlantic freshwater or hosing case, 1 Sv (1 Sv $\equiv 10^6$ m^3 s^{-1}) of freshwater is added to the ocean surface from 50° to 70°N in the Atlantic Ocean for 100 model years. In the second integration, the Antarctic freshwater or hosing case, a freshwater flux perturbation of 1 Sv is added to the ocean surface south of 60°S, also for 100 model years. After 100 yr, the additional freshwater flux is removed and the climate is allowed to recover in both experiments.

By comparing the two perturbation integrations to the control run, the effect of the freshwater forcing on the climate can be evaluated. Both atmospheric and oceanic responses are studied. It needs to be emphasized that this experimental design is strongly idealized. The freshwater inputs occur in a model simulation of present-day climate. It is likely that in the real world more land ice (and therefore a colder climate) is needed to obtain the large meltwater pulses used here and hence for the seesaw to operate. By comparing the hemispheric symmetry of the model response to the freshwater inputs, the seesaw hypothesis can be investigated.

2. Model description and experimental design

The AOGCM used in this study is fully described in Delworth et al. (2002) and compared with an older, lower-resolution model version in Dixon et al. (2003). The atmospheric model solves the equations of motion using a spectral rhomboidal truncation method for the prognostic variables where the number of waves retained is limited to 30. The transform grid is approximately 2.2° latitude by 3.75° longitude. It uses 14 unevenly spaced vertical levels. The atmospheric parameterizations are relatively simple: moist convective adjustment for convection processes in the atmosphere (Manabe 1969), simple mixing length theory for boundary layer and other mixing processes, relative humidity–based clouds (Manabe and Wetherald 1975), and a simple land surface scheme (Manabe 1969). This model has been called the Manabe Climate Model (MCM).

The oceanic component uses a grid system to solve its equations of motion. The grid spacing is the same as the atmosphere in the north–south direction (2.2°) and half the atmosphere in the east–west direction (1.875°). It uses 18 unevenly spaced vertical levels. Subgrid-scale mixing by eddies is parameterized by allowing mixing along isopycnal surfaces (Redi 1982; Tziperman and Bryan 1993).

Sea ice is allowed to move with the ocean currents unless the thickness is greater than 4 m, beyond which only divergent motions are allowed. A heat balance

between the top oceanic grid box and the sea ice is performed for each ocean component time step so that the ocean temperature under sea ice is exactly freezing (−2°C). No leads in the sea ice are allowed within a given grid box.

Over the continents whenever the "soil bucket" (Manabe 1969) overflows, the excess water is routed to the ocean using a river-routing scheme that is based the observed river drainage patterns. The coupled model uses monthly flux adjustments of heat and water (Manabe and Stouffer 1988). These adjustments are computed before the coupled model starts and are identical for all experiments described below. These adjustments help prevent large drifts of the coupled system away from observed values in the control integration.

We compare three integrations of the coupled model. In the first one, the water fluxes at the ocean surface in the North Atlantic Ocean, 50°–70°N, are modified by adding an external source of freshwater to the local freshwater fluxes that sums to 1 Sv. The external freshwater flux is held fixed for 100 model years. After that time, the additional freshwater input is removed and the climate is allowed to recover. The rate of 1 Sv is comparable to the total river flow in the present-day climate. As the land ice melted at the end of the last ice age, meltwater rates as large as our assumed value have been estimated; however, they did not last as long as our idealized flux (e.g., MacAyeal 1993; Clarke et al. 2003). The rate of 1 Sv applied for 100 yr would yield a globally averaged sea level rise of about 9 m (uncorrected for thermal expansion, if the thermal regime happens to change). In the model, the ocean component is constructed using the so-called rigid lid and virtual salt flux assumptions (Bryan 1969; Griffies et al. 2001); therefore, sea level does not change. This integration will be called the North Atlantic freshwater perturbation (or hosing) integration.

In the second integration, 1 Sv of freshwater is added to the Southern Ocean surface south of 60°S. Again, this rate is held fixed for 100 model years and then removed. This integration is called the Antarctic or SH freshwater perturbation (or hosing) integration. The third integration is a control, where the surface freshwater fluxes are not modified. The two perturbation simulations start from differing points in the control integration, about 500 to 700 model years from the start of the control integration. It is assumed that the differences in the results caused by the differences in the initial conditions are very small compared to the very large response to the freshwater perturbations. The control integration has been time integrated for more than 2000 model years.

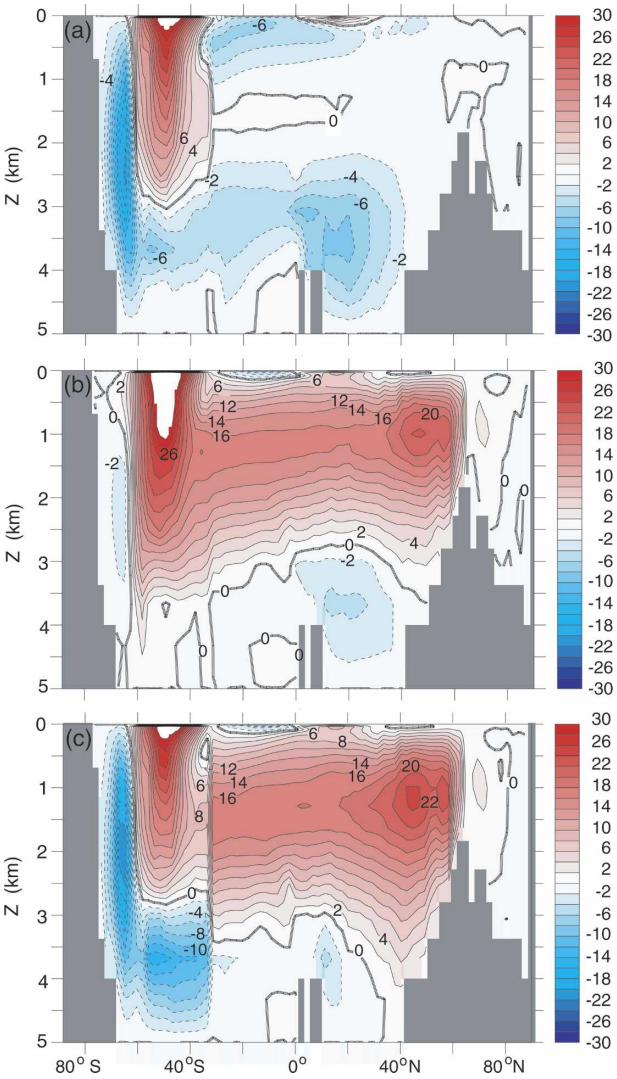

FIG. 1. Latitude–depth section of the streamfunction in the Atlantic Ocean. The values south of 30°S represent the global streamfunction values. The contour interval is 2 Sv. Red shading denotes positive values; blue negative values. (a) The 20-yr annual mean time average taken from the end of the freshwater input period in the North Atlantic. (b) The 20-yr annual mean time average taken from the end of the freshwater input period in the Southern Ocean. (c) The 100-yr annual mean time year average from the control.

3. Results

In general agreement with most previous studies, when freshwater is added to the ocean surface in one hemisphere, the THC weakens in that hemisphere (Fig. 1). In the control integration (Fig. 1c), the North Atlantic overturning maximum, which is located near 55°N and 1.3-km depth, is about 22 Sv. This is on the high side of the observed estimates (e.g., Macdonald and Wunsch 1996; Bryden and Imawaki 2001). The out-

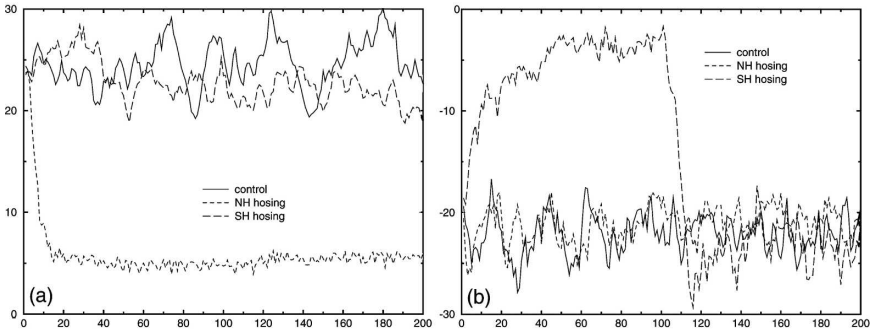

FIG. 2. (a) Maximum value of the streamfunction in the North Atlantic Ocean (Sv). This represents the North Atlantic THC. (b) Minimum value of the streamfunction south of 60°S.This represents the Antarctic THC. Solid line: control. Short dashed line: North Atlantic freshwater case. Long dashed line: Antarctic freshwater case.

flow from the Atlantic at 30°S is about 16 Sv. Again, this value is on the high side of the observed estimates. The cell that is found in the Antarctic bays is about 22 Sv. This cell represents the Antarctic merdional overturning and produces the AABW in the model. The observed AABW formation estimates are near 20 Sv (Ganachaud and Wunsch 2001).

In the North Atlantic freshwater case (Fig. 1a), the maximum overturning and the flow at 30°S is near 0 Sv by the end of the freshwater perturbation period, indicating that the Atlantic THC has stopped or is very weak. A reverse cell has developed in the upper ocean of the South Atlantic. Analysis indicates that this cell acts to transport freshwater into the Atlantic basin, allowing the THC to change stable states in this case (Manabe and Stouffer 1999; Gregory et al. 2003; Stouffer et al. 2006). The Antarctic overturning cell in the North Atlantic freshwater case remains near its initial 22-Sv strength. By the end of the freshwater perturbation period in the Antarctic freshwater case, the North Atlantic maximum is about 22 Sv. The flow at 30°S is about 16 Sv—very close to the control integration values, indicating little change. However, the cell in the Antarctic bays is very weak, about 2–3 Sv. This indicates that the Antarctic overturning cell is very weak and that the export of AABW may have stopped.

To show the time evolution of the overturning changes, two indices are constructed based on the meridional overturning cells seen in the control integration (Fig. 1c). The first index is of the maximum overturning value in the North Atlantic Ocean. It is computed by searching for the maximum positive overturning value in the North Atlantic from near the surface to the bottom of the ocean. In very weak or collapsed THC cases, this computation can find the bottom of the wind-driven cell in the North Atlantic. This problem will be discussed more below. In the construction of the Southern Ocean index, the computation searches for the most negative value of the overturning streamfunction south of 60°S from near the surface to the bottom of the ocean. In this case, this circulation index represents the rate of bottom water formation and export (AABW) in this model. In Fig. 1b, one notes that the overturning is very weak in the Antarctic freshwater case, indicating that the bottom water formation is nearly shut down. The problems with the indices noted above are indicative of the problems associated with the construction of many indices. Here they are used as a gross measure of the time-varying changes in the flows seen in Fig. 1.

The time series of streamfunction in the Atlantic and Antarctic Oceans for the North Atlantic freshwater case (Fig. 2) shows that within 20 yr of the start of the freshwater perturbation the Atlantic THC reaches a very low value (Fig. 2a). As seen in Fig. 1, the Atlantic THC is very weak by the end of the hosing period. Figure 2 indicates that after the first 20 model years, the Atlantic THC is very weak in the North Atlantic freshwater case. As noted above, the algorithm used to compute this index is not finding the true value of the overturning part of the circulation (see Fig. 1a). This is the reason that the minimum value in this time series is not closer to 0 Sv. The NH freshwater input has a very small or no impact on the Antarctic overturning cell (Fig. 2b).

When the freshwater is added to the Southern Ocean region, the Antarctic overturning cell associated with AABW production weakens to a small value (Fig. 2b). However, it takes more than 50 model years to reach this small value. After the addition of freshwater stops, the Antarctic cell rapidly recovers to near its original value. During the Antarctic freshwater perturbation, the Atlantic THC initially strengthens in the first 40 yr or so, although this may be just internal variability (Fig. 2a). Beyond year 80, the Atlantic THC is slightly weaker in the Antarctic freshwater case than in the

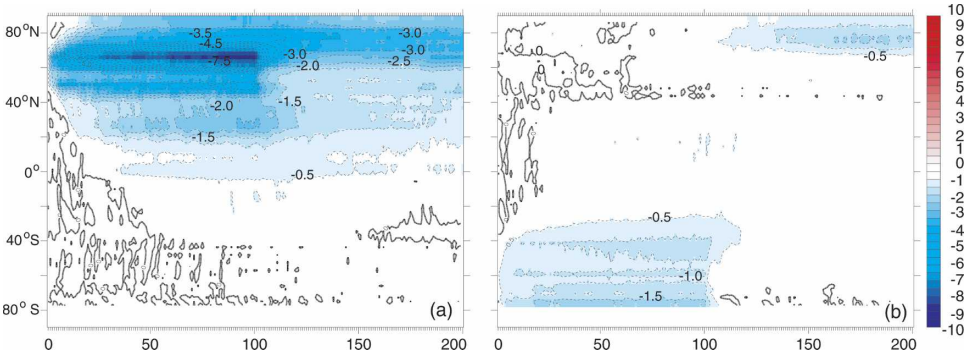

FIG. 3. Zonally averaged, annual mean sea surface salinity difference (PSU) computed by subtracting each individual year of the perturbation integration from its corresponding 200-yr time average from the control integration. Blue shading indicates negative values. (a) North Atlantic freshwater case. (b) Antarctic freshwater case.

control. This is due to an influx of fresher water from the SH. The spreading of the freshwater anomaly throughout the surface of the World Ocean is discussed below.

It is interesting that the Antarctic overturning cell seems to be more resistant to additional freshwater input than the Atlantic THC. However, it should be noted that the local freshwater fluxes are smaller in the Antarctic freshwater case than the North Atlantic fluxes because the hosing area in the North Atlantic is significantly smaller. In the North Atlantic case, the additional fluxes are concentrated from 50° to 70°N over a relatively narrow longitude span. In the Southern Ocean, the hosing region is south of 60°S, but it spans all longitudes.

The weakening of the overturning in the impacted hemisphere is because the surface water becomes fresher and therefore less dense. The relatively less dense waters cannot sink to depth. As the deep convection and overturning weaken, the residence time of surface waters in the region with the additional freshwater flux increases, and these waters become increasingly fresh (Fig. 3). In the North Atlantic freshwater case (Fig. 3a), near 70°N the sea surface salinity difference from the control is as large as 9.5 PSU by the end of the additional freshwater input. One notes little response in the Southern Hemisphere. In the Antarctic freshwater case (Fig. 3b), the magnitude of the sea surface salinity response is much less than in the Atlantic freshwater case, about 2 PSU freshening.

Two features are noted in the sea surface salinity for the Antarctic freshwater case, which are not seen in the North Atlantic case. One feature is the rapid recovery of the sea surface salinity in the Antarctic freshwater case after the freshwater perturbation is stopped (after 100 yr of hosing; Fig. 3b). This is not the situation for the North Atlantic freshwater case (Fig. 3a), where the sea surface salinity remains very fresh long after the additional freshwater perturbation is stopped. The recovery (or not) of the Atlantic THC in North Atlantic freshwater perturbation experiments is very model dependent (Stouffer et al. 2006). It is unclear if the real ocean has more than one stable equilibrium with present-day forcing.

The second feature is the spreading of the freshwater anomaly into the Northern Hemisphere in the Antarctic freshwater case (Fig. 3b). To investigate this issue further, Fig. 4 is constructed. In both of the freshwater input cases, the fresh anomaly is initially located near the region of the freshwater input (Fig. 4, top row). By the end of the hosing period in the North Atlantic freshwater case (Fig. 4, lower right), the negative salinity anomaly has spread throughout the Atlantic Ocean and into the North Pacific Ocean via the Bering Straits. There is also a fresh anomaly located near the warm pool in the western tropical Pacific, which appears to be a response to a shift in the ITCZ associated with the temperature changes in the NH (Stouffer et al. 2006). A key region is the Southern Ocean where the anomalies are relatively small and therefore do not impact the Antarctic overturning cell as noted above. In the Antarctic freshwater case (Fig. 4, lower left), the fresh salinity anomaly has spread throughout much of the World Ocean. In the high latitudes of the North Atlantic Ocean, the freshwater anomaly acts to inhibit the sinking branch of the Atlantic THC. This represents a clear asymmetry in the oceanic response to NH versus SH freshwater inputs.

The large difference in the local sea surface salinity response (local to the freshwater input) is at least partly due to the geometry of the Atlantic basin as discussed above. In the Southern Ocean, the additional freshwater input occurs at all longitudes. In the Atlantic freshwater input case, the input occurs only over approxi-

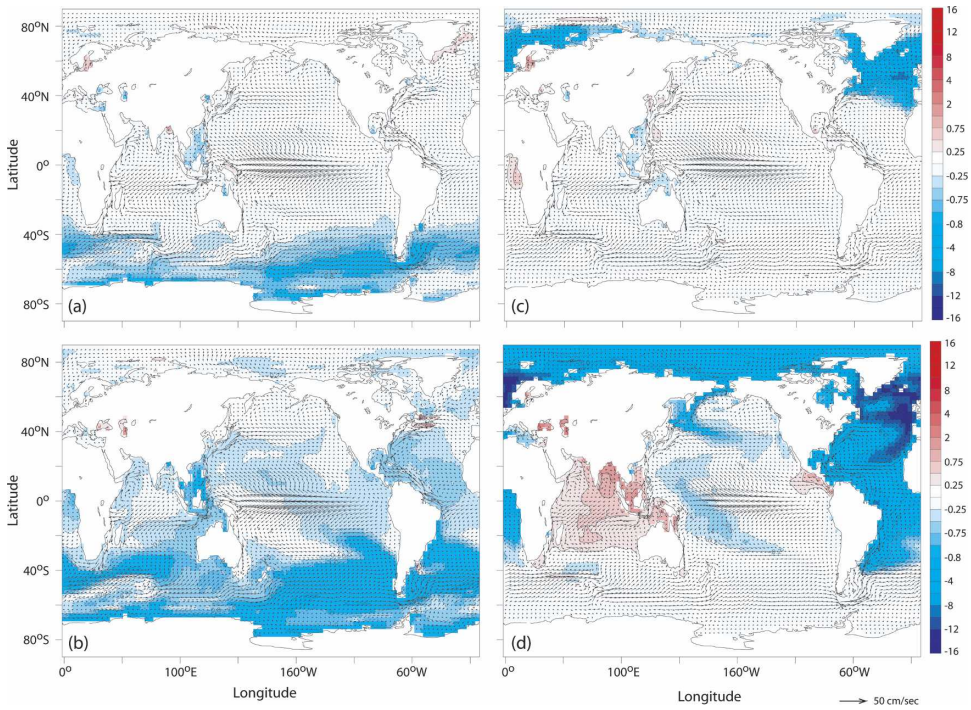

FIG. 4. Geographical distribution of SSS difference (PSU); Antarctic freshwater case minus control (100-yr average). (a), (c) Years 1 to 10 of the freshwater input. (b), (d) Years 91 to 100 of the freshwater input. Contour interval is 0.25 PSU. Blue shading indicates fresher water in the freshwater perturbation case (negative values). Vectors indicate surface flow in pertubation integration.

mately 60 degrees of longitude. The smaller hosing area intensifies the forcing (i.e., the size of the local freshwater perturbation) in the North Atlantic freshwater case. Also, since there is little ocean outside of the Atlantic basin at 65°N, the zonally averaged response can appear quite large, but only represents a relatively small fraction of the area at that latitude.

When freshwater is added to the ocean in high latitudes, it inhibits the local ocean convection and slows the overturning, cooling the surface waters and warming the subsurface waters (Figs. 5a,b). The subsurface warming is a maximum near the region where the freshwater perturbation is added. It extends from near the ocean surface to the ocean bottom. Some surface warming is also seen in the opposite hemisphere to the freshwater input. In the hemisphere with the freshwater perturbation, the surface cooling penetrates to depth in the middle-latitude region where the near-surface waters are subducted along the isopycnals making the intermediate water masses.

As described in the introduction, if the Atlantic THC weakens, the northward heat transport decreases (Fig. 6) in response to the freshwater input in the Atlantic. The weakening of the northward heat transport leads to a cooling in the NH and a slight warming of the SH as shown below. In the Antarctic freshwater case, the northward heat transport strengthens slightly in the Northern Hemisphere and to a greater extent in the Southern Hemisphere.

In the control integration, there is a relatively large trend in the globally averaged ocean temperature (Fig. 7). Trends of this magnitude for this variable are fairly common in AOGCM control integrations. The trends are evidence of the long time scales found in the ocean (Stouffer 2004) and problems with initializing AOGCMs in general (Stouffer and Dixon 1998). In both freshwater perturbation integrations, the ocean warms in response to the freshwater input in high latitudes. This warming is related to the capping of the ocean surface by freshwater. This inhibits the vertical mixing of heat in high latitudes, effectively trapping some of the oceanic heat and warming the ocean interior.

Interestingly, the rate of oceanic warming in the Antarctic freshwater case is about half as large as in the North Atlantic freshwater case. It is unclear why the rates of warming during the freshwater perturbation period are different, since the change in the deepwater formation rates are similar. During the period after the freshwater perturbation, the overturning in the Antarc-

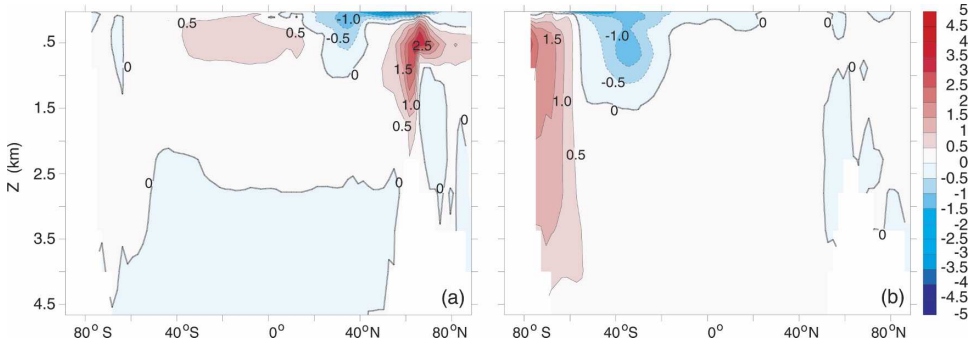

FIG. 5. Latitude–depth zonally and annually averaged ocean temperature difference (K) computed by subtracting the 20-yr time average at the end of the freshwater input from the corresponding 100-yr time average from the control. The contour interval is 0.5 K. Blue shading indicates negative values. (a) North Atlantic freshwater case and (b) Antarctic freshwater case.

tic perturbation rapidly recovers, allowing the oceanic heat to "escape" to the atmosphere. In the North Atlantic perturbation case, the Atlantic THC does not recover, leading to a larger oceanic heat uptake.

The relatively large warming at depth under the location of the additional freshwater fluxes causes a large local increase in sea surface height (Fig. 8). All of the changes in sea surface height presented here are only due to temperature and salinity changes and changes in the ocean circulation. The additional freshwater from the melting land ice (either from the freshwater perturbation or from melting land ice as a potential climate response) is not included in this figure by construction. In the North Atlantic freshwater case, the zonally averaged sea level rise is as large as 70 cm near 65°N. In the Antarctic freshwater case, the sea level increase is as large as 50 cm in the Antarctic Seas. Again in this case, one notes the relatively fast local recovery of the sea level after the hosing stops.

The SAT response to the addition of freshwater is remarkably symmetric (Fig. 9) between the two freshwater cases. In the hemisphere with the freshwater perturbation, there is a large cooling (5–6 K) of the zonally averaged SAT in the latitudes with the hosing. There is a small warming (0–2 K) in the opposite hemisphere. This pattern is remarkably similar for the Northern and Southern Hemisphere freshwater cases during the hosing period.

In both cases, the opposite hemisphere experiences a small warming almost as soon as the hosing starts. It takes about a decade for the cooling to reach its maximum. The symmetry of the SAT response between the two cases breaks down after the freshwater perturba-

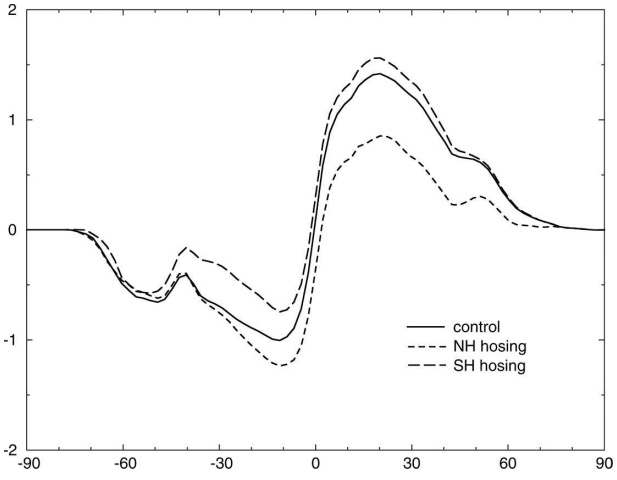

FIG. 6. Global northward heat transport (PW) for the last 20 yr of the freshwater perturbation integrations and a 100-yr period in the control. Solid line: control. Short dashed line: North Atlantic freshwater case. Long dashed line: Antarctic freshwater case.

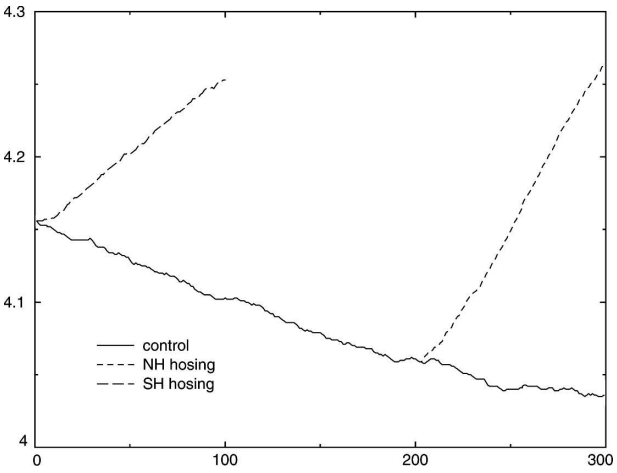

FIG. 7. Globally averaged, volume-averaged ocean temperature (K). Solid line: control. Short dashed line: North Atlantic freshwater case. Long dashed line: Antarctic freshwater case.

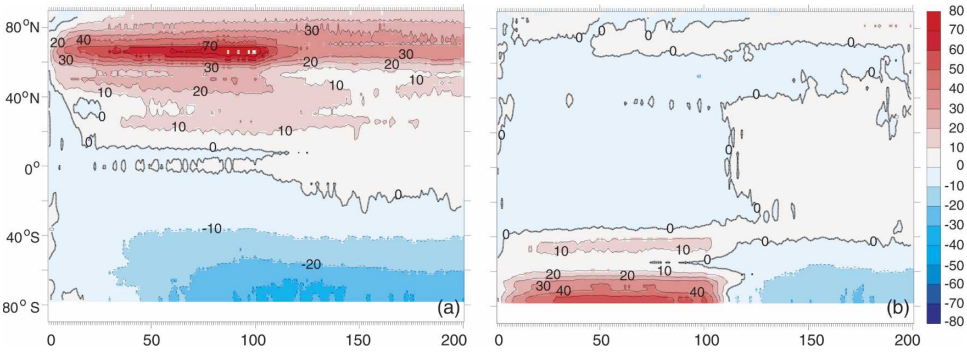

FIG. 8. Zonally averaged, annual mean sea surface height difference (cm) computed by subtracting each individual year of the perturbation integration from its corresponding 200-yr time average from the control integration. Blue shading indicates negative values. (a) North Atlantic freshwater case and (b) Antarctic freshwater case.

tion stops. In the Antarctic freshwater hosing case, the SAT quickly recovers after the hosing stops, while that is not the situation in the North Atlantic freshwater case.

An interesting question is if there is a time lag between the freshwater perturbation and the warming in the opposite hemisphere. Stocker and Johnsen (2003), using a simple thermodynamic model, find that a time lag of about 1000 yr between the NH and SH ice records produces the best fit to the curves. The integrations presented here are too short to fully address this question, and the interpretation is further complicated by the fact that the THC apparently changes stable states in the North Atlantic freshwater case and not in the Antarctic case. Therefore, it seems worthwhile to closely inspect Fig. 9, hopefully gaining some insight into this question.

As noted above, the maximum zonally averaged SAT change in the hemisphere with the freshwater perturbation occurs about 10 model years after the start of the hosing. Inspection of the SAT changes obtained from individual model grid points located near the ice core sites in Greenland and Antarctica (not shown) indicates that the local anomaly time scales are very similar to the zonal averages. In the hemisphere opposite the freshwater perturbation, the warming occurs more slowly. It is difficult to determine if the warming has reached a maximum by the end of the integrations. Longer integrations are needed to more fully address this issue.

In response to the freshwater perturbation, the hemisphere with the hosing cools and the precipitation decreases (Fig. 10). In the opposite hemisphere there is a slight warming and the precipitation increases slightly. Because of the relative changes in the two hemispheres, the interhemispheric temperature gradient changes. The ITCZ tends to move away from the cooler hemisphere and toward the warmer hemisphere (Broccoli et al. 2006). The shift of the ITCZ toward the warmer hemisphere is seen in both hosing cases.

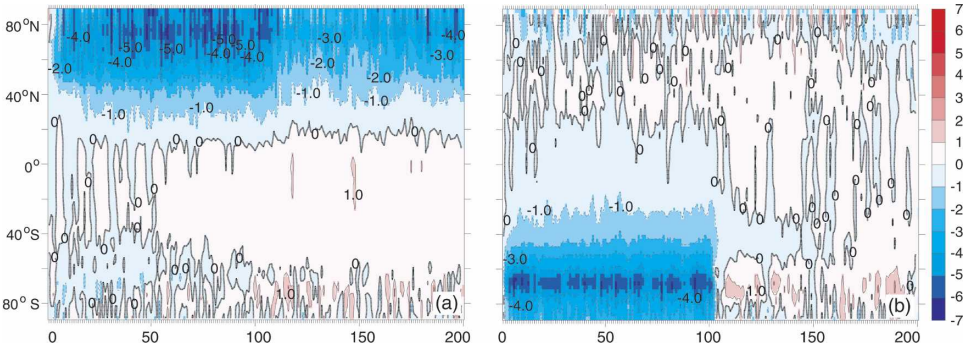

FIG. 9. Zonally averaged across all longitudes, the annual mean surface air temperature difference (K) computed by subtracting each individual year of the perturbation integration from its corresponding 200-yr time average from the control integration. Blue shading indicates negative values. (a) North Atlantic freshwater case and (b) Antarctic freshwater case.

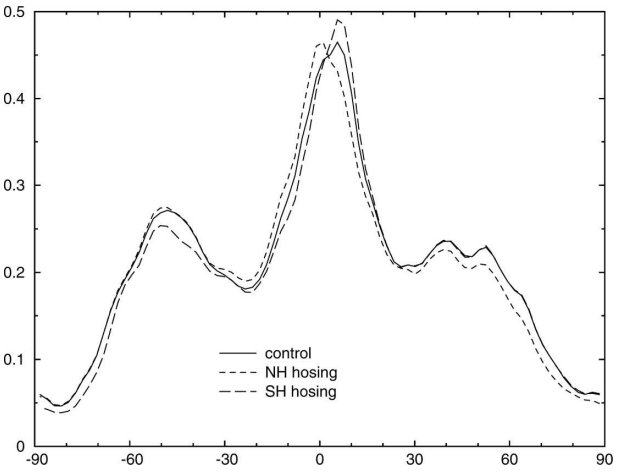

FIG. 10. Plot of zonally averaged, annual mean precipitation (cm day^{-1}) from the last 20 yr of the hosing period. Solid line: control. Short dashed line: NH hosing. Long dashed line: SH hosing.

4. Discussion

If these simulations are correct, then the oceanic response in terms of SSS and THC recovery to North Atlantic freshwater perturbations is radically different than to Antarctic freshwater perturbations (Seidov et al. 2005). Remarkably, in spite of the differences in the spreading of the SSS anomaly, the atmospheric response is fairly symmetrical between the two freshwater cases. In the North Atlantic hosing case, the North Atlantic freshens and strongly cools. The Atlantic THC weakens and is likely to have changed stable states: from the on to the off mode. As noted, above whether or not a model has a stable off mode varies from model to model. In the Antarctic freshwater case, the surface waters cool and freshen, but the oceanic response is smaller than the North Atlantic freshwater case. As a result of this and potentially other factors, the Antarctic overturning cell weakens but does not change stable states. At this point, it is unclear if the Antarctic overturning cell has two stable states (on and off) in this climate model. This topic is beyond our goals here and may be the focus of future investigations. Since the Antarctic overturning cell did not change stable states, it quickly recovers to its original strength after the hosing stops.

There are at least two causes of the different initial THC responses and recovery in the Antarctic and North Atlantic freshwater cases; both have to do with the geometry of the earth's continents (Seidov et al. 2005). The first is that the magnitude of the local additional freshwater fluxes is larger in the North Atlantic case than in the Antarctic because of the smaller surface area where the fluxes are applied. The second reason is that the SSS anomalies do not remain in or near the location of the additional freshwater fluxes in the Antarctic case (in sharp contrast to the North Atlantic case).

In the Antarctic freshwater case, the SSS anomalies move away from Antarctica (Fig. 4) because of the divergence of the surface currents (Fig. 4) and spread into all the whole ocean basins. This divergence is driven by two factors. The main factor, which is present in all the integrations presented here, is the climatological surface westerly winds that surround the Antarctic continent. These winds produce divergence of the surface waters over much of the Southern Ocean (Fig. 4). The second reason for the divergence is in response to the freshwater hosing in the perturbation integrations. The addition of the freshwater perturbation causes the surface waters to become much less dense, leading to a tendency for anomalous surface currents, flowing away from the hosing area (Fig. 4). These two factors work together to produce surface divergence across the surface of the Southern Ocean in the Antarctic perturbation integration.

As the surface waters flow north into the southern Indian, Pacific, and Atlantic basins, much of the freshwater anomaly produced by the freshwater hosing remains trapped near the ocean surface (Fig. 11). The surface gyres and horizontal mixing then transport the freshwater anomaly toward the north (and into the NH) in both the Atlantic and Pacific basins (Fig. 4).

New ocean-only experiments using an experimental design and freshwater fluxes comparable to those used in this study produce results in agreement with the AOGCM results described here (Seidov et al. 2005). The North Atlantic and SH surface freshening in both models (ocean-only and AOGCM) show the same response—the North Atlantic freshening persists in or near the impact area, while the surface freshening in the Southern Ocean spreads over the entire World Ocean. In the ocean-only experiments, the THC response is also qualitatively similar to that shown here.

An additional reason for the THC weakening in the Atlantic Ocean might be the change in the density gradient between the Atlantic and Pacific Ocean basins. As the surface freshwater anomaly escapes the Southern Ocean, it leaks into the Atlantic Ocean more than in the Pacific Ocean, thus weakening the density contrast between the Atlantic and Pacific Oceans. This density contrast has been shown to be the key for maintaining conveyor-like global THC (Seidov and Haupt 2003, 2005; Saenko et al. 2004). However, more research is needed to confirm or reject this line of thinking.

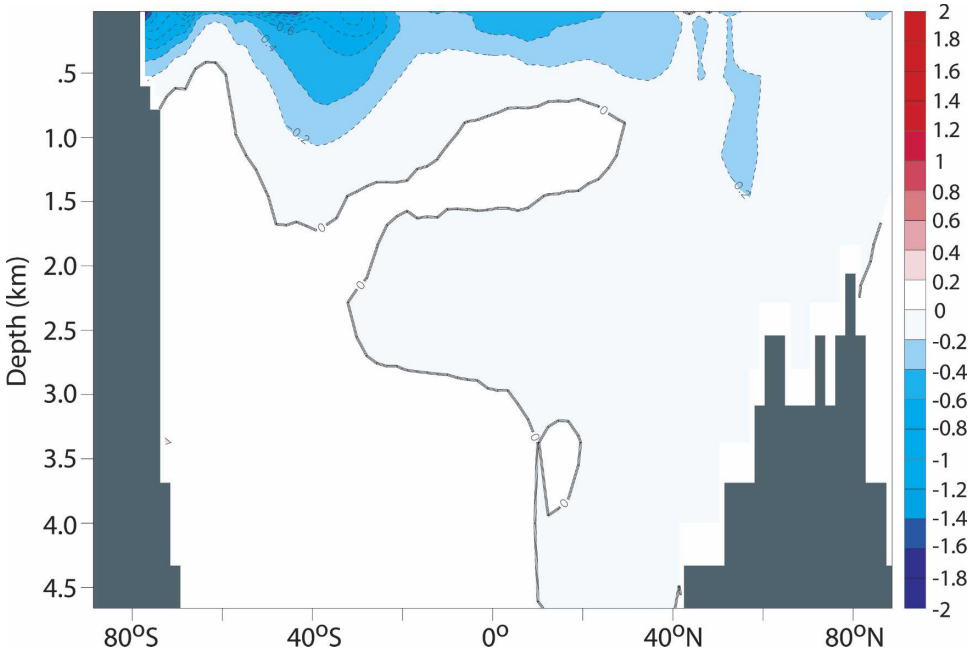

FIG. 11. Latitude–depth of the annually averaged salinity difference, years 76 to 100, of the Antarctic freshwater case minus a century time average from the control in the Atlantic basin. Units are PSU. Blue shading indicates values where the water is fresher in the perturbation case.

Finally, the differences between the results presented here and the Weaver et al. (2003) study need some additional discussion. As noted in the introduction, Weaver et al. found that the Atlantic THC changes stable states (off to on) by adding a freshwater perturbation north of the ACC in one experiment and near Antarctica in the second experiment. It would appear that these two studies yield very different THC responses to the Southern Hemisphere freshwater input. In the Weaver et al. case the THC strengthens, while in the results presented here, it weakens. However, since the initial Atlantic THC states are very different (on in this study, off in the Weaver et al. study), a direct comparison of the results is difficult. Investigating the response of the two models to common Southern Hemisphere freshwater forcings could be the subject of future studies.

5. Summary

We investigate the response of the AOGCM to freshwater perturbations in the North Atlantic and Southern Ocean. The experimental design is idealized where 1 Sv of freshwater is added to the ocean surface for 100 model years and then removed. In one case, the freshwater perturbation is located from 50° to 70°N in the Atlantic Ocean. In the second case, it is located south of 60°S in the Southern Ocean.

In the North Atlantic freshwater case, the Atlantic THC and associated northward heat transport weaken. In the Antarctic freshwater case, the Atlantic THC is mainly unchanged with a slight weakening toward the end of the integration (model year 200). This weakening is associated with the spreading of the fresh SSS anomaly from the Southern Ocean into the rest of the world's oceans. When the SSS anomaly reaches the high latitudes of the North Atlantic Ocean, it hinders the sinking of the surface waters, leading to the weakening of the THC.

The spreading of the fresh SSS anomaly from the Southern Ocean into the World Ocean surface waters is not seen in earlier ocean-only experiments (Seidov et al. 2001). In these experiments, the SSS anomaly is imposed, thereby preventing the anomaly from spreading by design. As noted above, in newer ocean-only experiments where the ocean-only forcing is freshwater water fluxes, the results are similar to those obtained from the AOGCM presented here. Given the geography of the SH and the fact that the surface winds and the ocean changes resulting from the intense local freshwater perturbation push the surface waters northward away from the Antarctic continent, it seems likely that the spreading of the SSS anomaly would occur in the real world. Having similar oceanic behavior in two different model types and using different approaches (OGCM driven by diagnosed freshwater fluxes and

self-consistent AOGCM) increase our confidence in the validity of our reasoning.

Because of the spreading of the SSS anomalies throughout the world's oceans, the time scale and exact locations and magnitudes of the freshwater inputs may be important in determining the climate response to SH freshwater perturbations. The key issue is the following: What would keep the freshwater SSS anomalies near the hosing region in the Southern Hemisphere (or at least confined to the Southern Ocean)? The spreading of the freshwater anomaly may produce far-afield changes in the ocean that could impact the climate response. The possible weakening of the Atlantic THC seen at the end of the Antarctic freshwater integrations is an example of a possible far-afield response. More realistic experimental designs are needed to explore this issue.

There is a remarkable symmetry in the atmospheric response between the two freshwater perturbation experiments. In both cases, the hemisphere with the freshwater perturbation cools and the opposite hemisphere warms slightly. In the zonally averaged SAT figures, both the magnitude and the zonally averaged pattern of the anomalies look similar between the two cases during the hosing period. After the SH hosing period, the Antarctic overturning cell and the associated climate changes rapidly recover toward the control integration values. In the Atlantic hosing case, the THC remains very weak and may have changed stable states—to an "off" mode.

The fact that the SAT (and that of other atmospheric fields) response is very symmetrical between the two freshwater cases leads to the possibility that the seesaw idea could be modified to include freshwater forcing from the SH as well as the NH (with the caveats noted above). The shutting down or slowing of the deepwater production in either hemisphere has the potential to produce a seesaw interhemispheric temperature response.

Acknowledgments. This study, through DS and BH, was supported in part by NSF Grant 0224605. Acknowledgment is also made to the donors of the ACS Petroleum Research Fund for partial support of this research, again through DS and BH (ACS PRF 36812-AC8). The authors thank R. Hallberg, J. Russell, J. Yin, R. Zhang, and two anonymous reviewers for comments that improved this manuscript.

REFERENCES

Blunier, T., and E. J. Brook, 2001: Timing of millennial-scale climate change in Antarctica and Greenland during the last glacial period. *Science,* **291,** 109–112.

Broccoli, A. J., K. A. Dahl, and R. J. Stouffer, 2006: The response of the ITCZ to Northern Hemisphere cooling. *Geophys. Res. Lett.,* **33,** L01702, doi:10.1029/2005GL024546.

Broecker, W. S., 1998: Paleocean circulation during the last deglaciation: A bipolar seesaw? *Paleoceanography,* **13,** 119–121.

——, 2000: Was a change in the thermohaline circulation responsible for the Little Ice Age? *Proc. Natl. Acad. Sci. USA,* **97,** 1339–1342.

Bryan, K., 1969: A numerical method for the study of the circulation of the World Ocean. *J. Comput. Phys.,* **4,** 347–376.

Bryden, H. L., and S. Imawaki, 2001: Ocean heat transport. *Ocean Circulation and Climate: Observing and Modelling the Global Ocean,* G. Siedler, J. Church, and J. Gould, Eds., Academic Press, 455–474.

Clark, P. U., N. G. Pisias, T. F. Stocker, and A. J. Weaver, 2002: The role of the thermohaline circulation and abrupt climate change. *Nature,* **415,** 863–869.

Clarke, G., D. Leverington, J. Teller, and A. Dyke, 2003: Superlakes, megafloods, and abrupt climate change. *Science,* **301,** 922–923.

Crowley, T. J., 1992: North Atlantic deep water cools the Southern Hemisphere. *Paleoceanography,* **7,** 489–497.

Cubasch, U., and Coauthors, 2001: Projections of future climate change. *Climate Change 2001: The Scientific Basis,* J. T. Houghton et al., Eds., Cambridge University Press, 525–582.

Delworth, T. L., R. J. Stouffer, K. W. Dixon, M. J. Spelman, T. R. Knutson, A. J. Broccoli, P. J. Kushner, and R. T. Wetherald, 2002: Review of simulations of climate variability and change with the GFDL R30 coupled climate model. *Climate Dyn.,* **19,** 555–574.

Dixon, K. W., T. L. Delworth, T. R. Knutson, M. J. Spelman, and R. J. Stouffer, 2003: A comparison of climate change simulations produced by two GFDL coupled climate models. *Global Planet. Change,* **37,** 81–102.

Ganachaud, A., and C. Wunsch, 2001: Improved estimates of global ocean circulation, heat transport and mixing from hydrographic data. *Nature,* **408,** 453–457.

Ganopolski, A., and S. Rahmstorf, 2001: Simulation of rapid glacial climate changes in a coupled climate model. *Nature,* **409,** 153–158.

Gregory, J. M., O. A. Saenko, and A. J. Weaver, 2003: The role of the Atlantic freshwater balance in the hysteresis of the meridional overturning circulation. *Climate Dyn.,* **21,** 707–717.

Griffies, S. M., R. C. Pacanowski, M. Schmidt, and V. Balaji, 2001: Tracer conservation with an explicit free surface method for *z*-coordinate ocean models. *Mon. Wea. Rev.,* **129,** 1081–1098.

Knutti, R., J. Fluckiger, T. F. Stocker, and A. Timmermann, 2004: Strong hemispheric coupling of glacial climate through freshwater discharge and ocean circulation. *Nature,* **430,** 851–856.

MacAyeal, D. R., 1993: Binge/purge oscillations of the Laurentide ice sheet as a cause of the North Atlantic's Heinrich events. *Paleoceanography,* **8,** 775–785.

Macdonald, A., and C. Wunsch, 1996: An estimate of global ocean circulation and heat fluxes. *Nature,* **382,** 436–439.

Manabe, S., 1969: Climate and the ocean circulation. Part I: The atmospheric circulation and the hydrology of the earth's surface. *Mon. Wea. Rev.,* **97,** 739–774.

——, and R. T. Wetherald, 1975: The effects of doubling CO_2 concentration on the climate of a general circulation model. *J. Atmos. Sci.,* **32,** 3–15.

——, and R. J. Stouffer, 1988: Two stable equilibria of a coupled ocean–atmosphere model. *J. Climate,* **1,** 841–866.

——, and ——, 1995: Simulation of abrupt climate change in-

duced by freshwater input to the North Atlantic Ocean. *Nature,* **378,** 165–167.

——, and ——, 1997: Coupled ocean–atmosphere model response to freshwater input: Comparison to Younger Dryas event. *Paleoceanography,* **12,** 321–336.

——, and ——, 1999: Are two modes of thermohaline circulation stable? *Tellus,* **51A,** 400–411.

Rahmstorf, S., 2002: Ocean circulation and climate during the past 120,000 years. *Nature,* **419,** 207–214.

Redi, M. H., 1982: Oceanic isopycnal mixing by coordinate rotation. *J. Phys. Oceanogr.,* **12,** 1154–1158.

Rind, D., P. deMenocal, G. Russell, S. Sheth, D. Collins, G. Schmidt, and J. Teller, 2001: Effects of glacial meltwater in the GISS coupled atmosphere–ocean model. *J. Geophys. Res.,* **106,** 27 335–27 353.

Saenko, O. A., A. Schmittner, and A. J. Weaver, 2004: The Atlantic–Pacific seesaw. *J. Climate,* **17,** 2033–2038.

Schmittner, A., O. A. Saenko, and A. J. Weaver, 2003: Coupling of the hemispheres in observations and simulations of glacial climate change. *Quat. Sci. Rev.,* **22,** 659–671.

Seidov, D., and M. Maslin, 2001: Atlantic Ocean heat piracy and the bi-polar climate sea-saw during Heinrich and Dansgaard-Oeschger events. *J. Quat. Sci.,* **16,** 321–328.

——, and B. J. Haupt, 2003: Freshwater teleconnections and ocean thermohaline circulation. *Geophys. Res. Lett.,* **30,** 1329, doi:10.1029/2002GL016564.

——, and ——, 2005: How to run a minimalist's global ocean conveyor. *Geophys. Res. Lett.,* **32,** L07610, doi:10.1029/2005GL022559.

——, E. J. Barron, and B. J. Haupt, 2001: Meltwater and the global ocean conveyor: Northern versus southern connections. *Global Planet. Change,* **30,** 253–266.

——, R. J. Stouffer, and B. J. Haupt, 2005: Is there a simple bipolar ocean seesaw? *Global Planet. Change,* **49,** 19–27.

Steig, E. J., and R. B. Alley, 2002: Phase relationships between Antarctica and Greenland climate records. *Ann. Glaciol.,* **35,** 451–456.

Stocker, T. F., 1998: The seesaw effect. *Science,* **282,** 61–62.

——, and S. J. Johnsen, 2003: A minimum thermodynamic model for the bipolar seesaw. *Paleoceangraphy,* **18,** 1087, doi:10.1029/2003PA000920.

——, D. G. Wright, and W. S. Broecker, 1992: The influence of high-latitude surface forcing on the global thermohaline circulation. *Paleoceanography,* **7,** 529–541.

Stouffer, R. J., 2004: Time scales of climate response. *J. Climate,* **17,** 209–217.

——, and K. W. Dixon, 1998: Initialization of coupled models for use in climate studies: A review. Research Activities in Atmospheric and Oceanic Modelling, Tech. Rep. 27, WMO/TD-865, World Meteorological Organization, Geneva, Switzerland, I.1–I.8.

——, and Coauthors, 2006: Investigating the causes of the response of the thermohaline circulation to past and future climate changes. *J. Climate,* **19,** 1365–1387.

Tziperman, E., and K. Bryan, 1993: Estimating global air–sea fluxes from surface properties and from climatological flux data using a ocean general circulation model. *J. Geophys. Res.,* **98,** 22 629–22 644.

Vellinga, M., and R. Wood, 2002: Global climatic impacts of a collapse of the Atlantic thermohaline circulation. *Climatic Change,* **54,** 251–267.

Weaver, A. J., O. A. Saenko, P. U. Clark, and J. X. Mitrovica, 2003: Meltwater pulse 1A from Antarctica as a trigger of the Bølling–Allerød warm interval. *Science,* **299,** 1709–1713.